Engineering Failure Analysis 29 (2013) 56–61

Contents lists available at SciVerse ScienceDirect

Engineering Failure Analysis

journal homepage: www.elsevier.com/locate/engfailanal

Failure analysis of a petrochemical plant reducing gear

Sandro Griza [a], Antônio Pereira Santos [a], Thiago Figueiredo Azevedo [a], Carlos Eduardo Fortis Kwietniewski [b], Afonso Reguly [b,*], Telmo R. Strohaecker [b]

[a] *Programa de Pós-Graduação em Ciência e Engenharia dos Materiais, Universidade Federal de Sergipe, São Cristóvão, Brazil*

[b] *Programa de Pós-Graduação em Engenharia de Metalúrgica, de Minas e Materiais, Universidade Federal do Rio Grande do Sul, Porto Alegre, Brazil*

ARTICLE INFO

Article history:
Received 26 September 2012
Received in revised form 1 November 2012
Accepted 22 November 2012
Available online 10 December 2012

Keywords:
Fracture mechanics
Fatigue
Crack growth
Stress concentration
Gear

ABSTRACT

This study aims to investigate the cause of failure of an 845 mm external diameter reducing gear that operated during 30 months in a petrochemical plant. The failure analysis procedure included material characterisation (microstructure, chemical composition and microhardness), fracture surface evaluation, and stress distribution by finite elements on critical regions of the gear. Fracture mechanics and fatigue crack growth were also used to develop a $da/dN–\Delta K$ curve and then determine the gear material crack growth resistance. Results indicate that the gear was not properly manufactured and failure occurred as a result of a fatigue process facilitated by a manufacturing defect.

1. Introduction

Gears are often subjected to severe service conditions and are one of the key components responsible for the transmission of movement. Frequently, high cyclic loading is imposed to gears and fatigue is an important concern. Gear designers also need to take into consideration wear, contact fatigue resistance and bending at gear tooth root [1–3]. Fatigue resistance can be determined using Wohler curves, where the material endurance limit is estimated for smooth samples. However, when the sample or even the component has a flaw, the fracture mechanics approach must be used [4]. Usually curves correlating the propagation rate and the stress intensity in the crack tip ($da/dN \times \Delta K$) are build to estimate the fatigue crack growth (FCG) resistance and in some cases can also give the fatigue threshold (ΔKth). In the fracture mechanics approach, the component geometry is fundamental, since stress concentration can rise significantly, increasing the crack growth rate. Therefore, it is crucial that components subjected to fatigue have been designed in such way that stress concentrators are avoided.

This investigation aims to point out the reasons that caused the failure of an 845 mm diameter reducing gear that operated during 30 months. The gear was part of the main polypropylene extruder of the company with the total cost of the failure estimated in around U$ 460,000 dollars. Fig. 1 shows a general view of the fractured gear. The fatigue crack propagated tangentially to the longitudinal plane of the gear resulting in the separation of three gear teeth. The failure analysis included a closed observation of the gear design, its material characteristics (chemical composition, microstructure and hardness), and stress distribution analysis within critical regions of the gear. Fracture mechanics applied to fatigue was also used to determine the FCG rate as well as the fatigue threshold.

* Corresponding author. Tel.: +55 51 3308 3551; fax: +55 51 3308 3565.
E-mail address: reguly@ufrgs.br (A. Reguly).

1350-6307/$ - see front matter © 2012 Elsevier Ltd. All rights reserved.
http://dx.doi.org/10.1016/j.engfailanal.2012.11.013

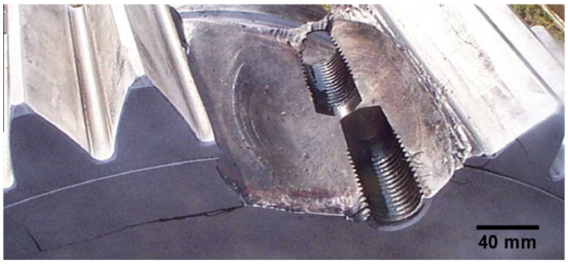

Fig. 1. General view of the fracture surface of the spur gear.

2. Experimental procedure

2.1. Material characterisation

In order to access the conformity of the gear to the design specification chemical analysis, hardness and microstructural evaluation were performed. The chemical composition was evaluated at the core of the gear using an optical spectrometer Spectra – Spectrolab. Vickers hardness profile was taken with 500 g load with 0.05 mm increments from the surface of the tooth to the core. Optical microscopy was used to evaluate the case and core microstructure.

2.2. Fracture examination

The fracture surface of the gear was examined by both naked eye and stereo microscope in order to determine the fracture initiation point and the general fracture surface characteristics.

2.3. Stress analysis

Fig. 2 shows a basic drawing of the fractured gear. The design project included several holes for handling and transport of the large gear. Those holes where placed 90° apart and a perfect alignment between matching holes were not achieved as can be seen in Fig. 2c.

Stress distribution within the gear was determined by the finite elements method. A solid with dimension of the gear was generated including two of the machined holes used for the gear handling. The intersection between the two holes resulted in an elliptical flaw with a larger diagonal of approximately 6 mm. For the modeling the gear was restricted by its inner diameter. The load applied on modeling was derived from the gear operating torque. It was distributed over three teeth adjacent to the flaw and applied in the pressure line direction on a surface of 3670 mm^2 over each the three teeth, so that the tooth just above the flaw experienced a stress of 80 MPa, and its neighboring teeth experienced stresses of 65 MPa. A tetragonal quadratic mesh was used in the simulation with a mesh refinement applied at the region of the defect as shown in Fig. 3.

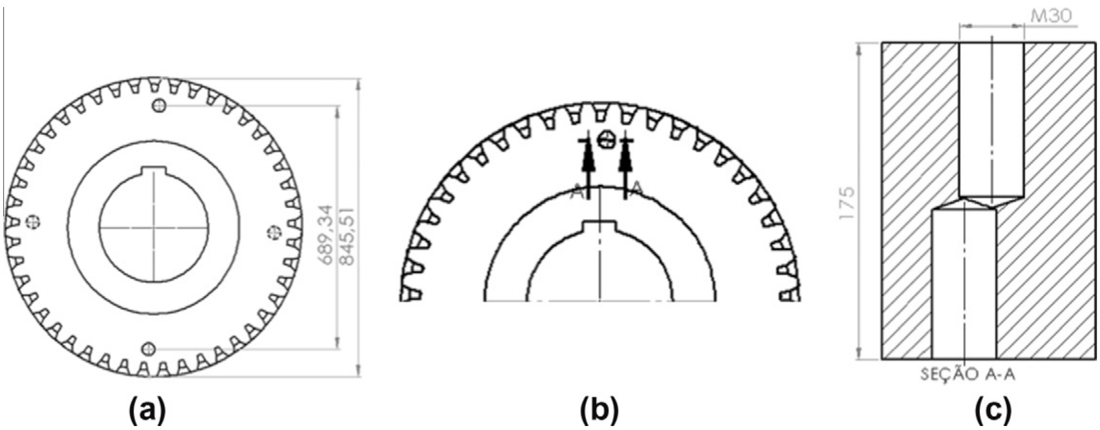

Fig. 2. General dimension of the spur gear. (a) Positioning of the holes for handling the gear, (b) location of the holes adjacent to fracture surface, (c) alignment between matching holes at the fracture.

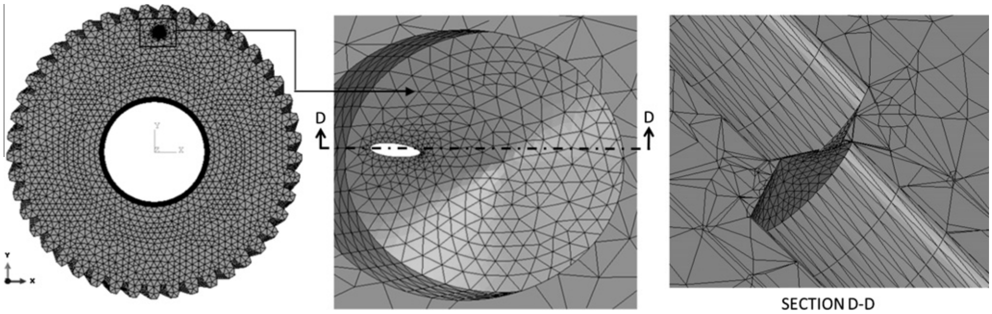

Fig. 3. General representation of the mesh used in the modeling with a detailed view of the defect region.

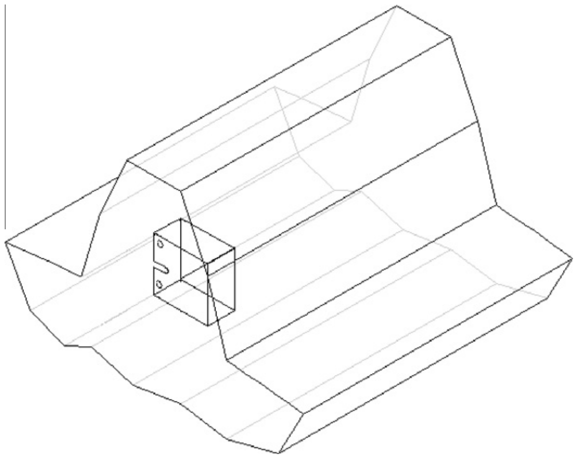

Fig. 4. Position of the specimens machined from the fractured gear.

To determine the stress intensity factor (SIF) for the crack tip the defect was considered much smaller than the gear (semi-infinite body) and type I loading mode was considered. With this consideration the SIF can be described as a function of applied load (σ) and defect dimension (a) according to the following equation:

$$K = \sigma\sqrt{\pi a} \tag{1}$$

2.4. Fatigue crack growth rate

FCG tests were conducted in accordance with the ASTM E647 [5] test method using compact tension specimens with thickness (B) of 15 mm and width (W) of 30 mm machined from the core of fractured gear. Fig. 4 shows the plane of the gear teeth from where the FCG specimens were machined. Both fatigue pre-cracking and the FCG tests were performed in a MTS 810 servo hydraulic. Load decreasing up to a crack growth rate of 10^{-9} m/cycle was used to determine the fatigue threshold. For the fatigue crack growth testing a loading ratio $R = 0.1$ was used.

3. Results and discussion

3.1. Material characterisation

Table 1 shows the chemical composition of the material used to fabricate the reducing gear. After machining, the gear was carburized, quenched and tempered. The final microstructure was tempered high carbon martensite at the case with a mixture of bainite and low carbon martensite at the core (Fig. 5). The microhardness profile shown in Fig. 6 indicated an effective case depth of 3.1 mm which is in accordance with the specification for this component.

3.2. Fracture surface observation

A closer examination of the fracture surface indicates that the fatigue crack has nucleated at the intersection of two machined holes used for handling the gear. From Fig. 7, it was also possible to observe that after nucleation, the cracks have

Table 1
Chemical composition of the reducing gear material (wt%).

C	Si	Mn	Cr	Ni	Cu	Mo	S	P
0.20	0.23	0.80	1.17	0.01	0.02	0.21	0.011	0.010

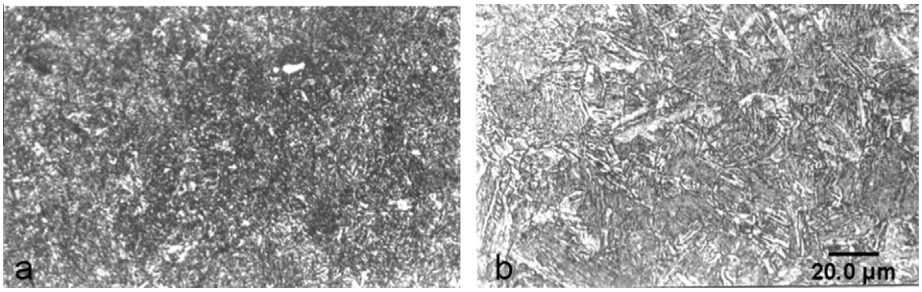

Fig. 5. Representative microstructure observed for the gear tooth. (a) Case – high carbon tempered martensite with dispersed carbides, (b) core – low carbon tempered martensite and bainite. MO. Etchant 2% Nital.

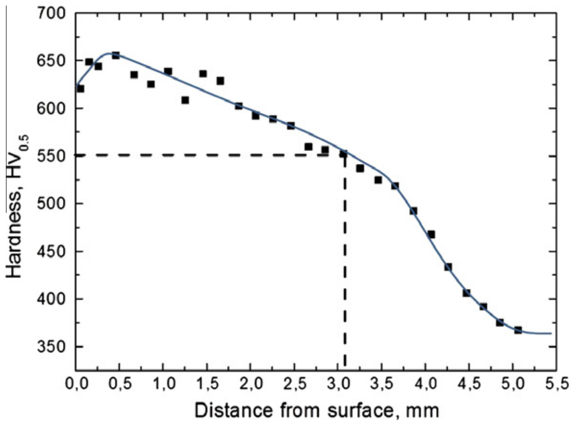

Fig. 6. Vickers hardness profile from gear tooth surface to core.

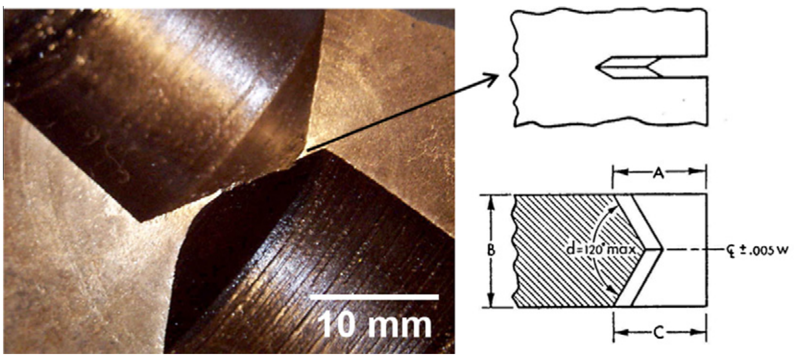

Fig. 7. Closer view of the fracture surface highlighting the Chevron notch like defect. Two crack initiation fronts can be observed at the intersection of the machined holes.

propagated by fatigue as indicated by beach marks. Two crack propagation fronts can be observed: one along the direction in which the gear rotates and the other propagating against the gear rotation direction. The initial machined flaw has worked as a stress concentrator resembling a Chevron notch, which is indicated by ASTM E-399-90 [6] procedure to facilitate the creation of fatigue pre-cracks (Fig. 7).

According to the gear producer this failure was a result of loading in excess of design limit because the calculated stresses at the crack initiation region where below the fatigue limit of the material. Using the Wohler curves approach for notched samples, it seems that the service loading conditions would not be severe enough to nucleate a fatigue crack. However, the poor matching of the two machined holes promoted the creation of a 6 mm elliptical flaw. In this case, Wohler curves no longer can be used to determine fatigue resistance and the fracture mechanics approach must be use.

3.3. Fatigue crack grow rate

Fig. 8 shows the fatigue crack grow rate curve for compact tension specimens extracted from the fractured gear. The Paris law parameters ($da/dN = C\Delta K^{m}$) as well as fatigue threshold (ΔKth = 4.3 MPa m$^{1/2}$) are presented.

3.4. Stress analysis

Finite element modeling indicates stresses in the order of 703 and 200 MPa at crack initiation points (Fig. 9). These stress differences at both singularity ends are due to their geometry differences. As can be seen in Fig. 9, the 703 MPa arise from a sharp wall resulting from the cone intersection, whereas the 200 MPa occur in a section with a thicker wall. Eq. (1) can be applied to this case if one considers the defect much smaller than the gear (semi-infinite body) and that a mode I type can be used to describe the loading mode. Applying the 200 MPa stress to Eq. (1) with a defect geometry a = 3 mm, one can obtain a ΔK = 19.4 MPa m$^{0.5}$ (load ranging from max. load = 200 and 0 MPa). According to Fig. 8 for this ΔK value the material is in the stable crack growth region indication fatigue crack propagation for this condition. Even higher stresses, 703 MPa, were obtained at the other initiation point but a rapidly decrease in this load is expected once the sharp interface between holes is crossed.

The gear tooth geometry is usually the region that is more closely controlled during manufacture, this happens because the face and fillet geometry can greatly affect gear performance and are usually the place of failures [7–9]. However, as

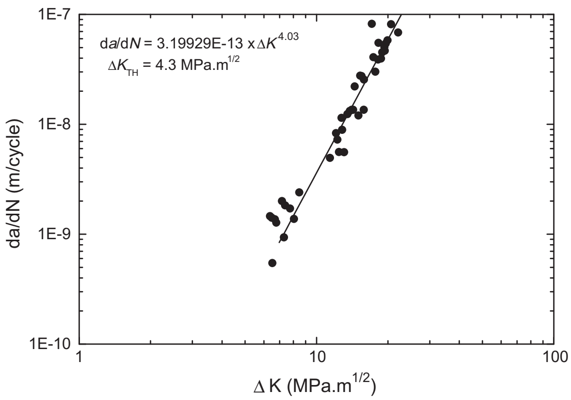

Fig. 8. Fatigue crack grow rate curve for compact tension specimens extracted from the fractured gear.

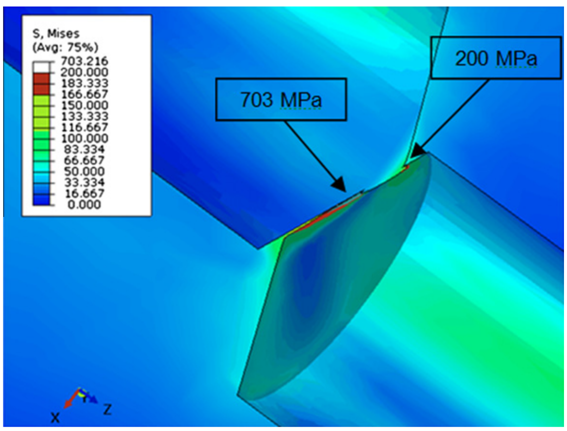

Fig. 9. Stress distribution along the end of the matching holes.

shown in this analysis, a poorly placed non-operational feature can induce local stress concentration and promote catastrophic failure.

4. Conclusions and recommendations

The failure occurred by fatigue facilitated by poorly designed holes drilled for shipping and handling the gear. The holes made on both sides of the gear were not aligned, and this produced an elliptically shaped defect which acted as a stress concentrator, promoting fatigue crack propagation in two fronts. The numerical simulations based on the geometry of the defect and service loads applied to the gear indicated that the stress intensity at the defect lies in the stable fatigue crack propagation region.

To prevent future failures, the adoption of an inspection plan after manufacturing that also consider the region of the holes is recommend. Furthermore, the position of the holes for handling the gear is too close to a region under the gear teeth where stresses are concentrated during gear operation. The possibility of slightly decreasing the 689 mm distance between hole centers (see Fig. 2) so that they move away from the region of higher stress should be evaluated. A reduction to 600 mm, for example, should not significantly alter the gear transportation logistics but would have a decisive influence in terms of the stress level at the singularity.

Acknowledgements

The authors would like to thank the financial support of CAPES, CNPq and FINEP.

References

[1] Moorthy V, Shaw BA. Contact fatigue performance of helical gears with surface coatings. Wear 2012;276–277:130–40.
[2] Glodež S, Šraml M, Kramberger J. A computational model for determination of service life of gears. Int J Fatigue 2002;24:1013–20.
[3] Kramberger J, Šraml M, Glodež S, Flašker J, Potrc I. Computational model for the analysis of bending fatigue in gears. Comput Struct 2004;82(23–26):2261–9.
[4] MackAldener M, Olsson M. Analysis of crack propagation during tooth interior fatigue fracture. Eng Fract Mech 2002;69:2147–62.
[5] ASTM E 647. Standard test method for measurement of fatigue crack growth rates. United States: ASTM International; 2008.
[6] ASTM E 399. Standard test method for linear-elastic plane-strain fracture toughness K_{IC} of metallic materials. United States: ASTM International; 2009.
[7] Fernandes PJL. Tooth bending fatigue failures in gears. Eng Fail Anal 1996;3:219–25.
[8] Chen Z, Shao Y. Dynamic simulation of spur gear with tooth root crack propagating along tooth width and crack depth. Eng Fail Anal 2011;18:2149–64.
[9] Fernandes PJL, McDuling C. Surface contact fatigue failures in gears. Eng Fail Anal 1997;4:99–107.